



Synthesis and biological evaluation of ^{18}F labeled fluoro-oligo-ethoxylated 4-benzylpiperazine derivatives for sigma-1 receptor imaging

Xia Wang^a, Yan Li^a, Winnie Deuther-Conrad^b, Fang Xie^a, Xin Chen^a, Meng-Chao Cui^a, Xiao-Jun Zhang^c, Jin-Ming Zhang^c, Jörg Steinbach^b, Peter Brust^b, Bo-Li Liu^a, Hong-Mei Jia^{a,*}

^aKey Laboratory of Radiopharmaceuticals (Beijing Normal University), Ministry of Education, College of Chemistry, Beijing Normal University, Beijing 100875, PR China

^bHelmholtz-Zentrum Dresden-Rossendorf, Institute of Radiopharmacy/Department of Neuroradiopharmaceuticals, 04318 Leipzig, Germany

^cNuclear Medicine Department, Chinese PLA General Hospital, Beijing 100853, PR China

ARTICLE INFO

Article history:

Received 8 August 2012

Revised 11 October 2012

Accepted 23 October 2012

Available online 31 October 2012

Keywords:

σ_1 Receptor

Fluoro-oligo-ethoxylated

4-Benzylpiperazine

F-18

ABSTRACT

We report the synthesis and evaluation of a series of fluoro-oligo-ethoxylated 4-benzylpiperazine derivatives as potential σ_1 receptor ligands. In vitro competition binding assays showed that 1-(1,3-benzodioxol-5-ylmethyl)-4-(4-(2-fluoroethoxy)benzyl)piperazine (**6**) exhibits low nanomolar affinity for σ_1 receptors ($K_i = 1.85 \pm 1.59$ nM) and high subtype selectivity (σ_2 receptor: $K_i = 291 \pm 111$ nM; $K_i\sigma_2/K_i\sigma_1 = 157$). [^{18}F]**6** was prepared in 30–50% isolated radiochemical yield, with radiochemical purity of >99% by HPLC analysis after purification, via nucleophilic $^{18}\text{F}^-$ substitution of the corresponding tosylate precursor. The $\log D_{\text{pH } 7.4}$ value of [^{18}F]**6** was found to be 2.57 ± 0.10 , which is within the range expected to give high brain uptake. Biodistribution studies in mice demonstrated relatively high concentration of radiotracers in organs known to contain σ_1 receptors, including the brain, lungs, kidneys, heart, and spleen. Administration of haloperidol 5 min prior to injection of [^{18}F]**6** significantly reduced the concentration of radiotracers in the above-mentioned organs. The accumulation of radiotracers in the bone was quite low suggesting that [^{18}F]**6** is relatively stable in vivo defluorination. The ex vivo autoradiography in rat brain showed high accumulation of radiotracers in the brain areas known to possess high expression of σ_1 receptors. These findings suggest that [^{18}F]**6** is a suitable radiotracer for imaging σ_1 receptors with PET in vivo.

© 2012 Elsevier Ltd. All rights reserved.

1. Introduction

Sigma-1 (σ_1) receptors represent a distinct class of intracellular membrane proteins whose C-terminus possesses chaperone activity.¹ They are predominantly expressed at the endoplasmic reticulum (ER) in a variety of cells and organs. It has been reported that σ_1 receptors translocate from the mitochondria-associated membrane to the cell nucleus or cell membrane and regulate several targets, including various ion channels, G-protein-coupled receptors, lipids, and other signaling proteins by a direct protein–protein interaction with another ER chaperone-binding immunoglobulin protein/78 kDa glucose-regulated protein (BiP/GRP-78).^{1,2} It is noteworthy that the chaperone activity can be manipulated by synthetic or endogenous ligands or by cations such as Ca^{2+} in a clear agonist-antagonist manner.^{1,3} More recent findings indicate that σ_1 receptors are important regulators in cellular morphology and neuronal plasticity.^{4,5} Although the molecular function of σ_1 receptors needs further elucidation, more and more evidence suggests that the σ_1 receptors are linked to a number of human dis-

eases, including brain disorders, tumors as well as heart failure.^{3,6–9} Therefore, they represent potential targets for treatment of these diseases.^{3,6} Development of σ_1 receptor ligands including agonists and antagonists could have wide therapeutic applications, while development of specific radiotracers for in vivo imaging of σ_1 receptors may provide useful diagnostic tools for investigation of their pathophysiology.

Many potential radiotracers for imaging σ_1 receptor expression with PET and SPECT have also been reported in the past few years. But until now, only a few tracers such as [^{11}C]SA4503,^{10,11} [^{18}F]FPS,¹² and [^{123}I]TPCNE¹³ have been evaluated in human studies. However, [^{18}F]FPS¹⁴ and [^{123}I]TPCNE¹³ were found to have irreversible kinetics. Many σ receptor ligands have affinity for the vesicular acetylcholine transporter (VACHT) and the emopamil binding protein (EBP).^{15–18} SA4503 was reported to show affinities for VACHT ($K_i = 50.2$ nM)¹⁵ and EBP ($K_i = 1.72$ nM).¹⁶ But [^{11}C]SA4503 did not seem to bind to VACHT in the rat brain in vivo.¹⁹ Recently, Toyohara et al. confirmed that the brain uptake of [^{11}C]SA4503 in mice was not blocked by high affinity EBP blockers tamoxifen (EBP $K_i = 2.8$ nM, $K_i\sigma_1/K_i\text{EBP} = 12$) and trifluoperazine (EBP $K_i = 3.9$ nM, $K_i\sigma_1/K_i\text{EBP} = 52$).²⁰ The newly developed compound [^{18}F]fluspidine showed weak affinity for VACHT

* Corresponding author. Tel./fax: +86 10 58808891.

E-mail address: hmjia@bnu.edu.cn (H.-M. Jia).

($K_i = 1400$ nM) and EBP ($K_i = 211$ nM).²¹ Selectivity toward these binding sites should be taken into consideration when designing new selective ligands, although the relationship between the σ receptor and EBP has not been clearly elucidated.

In our previous work, we have reported that [¹²⁵I]BP-I showed high binding affinity for σ_1 receptors and high selectivity to the σ_2 receptor subtype in vivo.²² Since imaging with PET has many advantages over SPECT such as higher detection sensitivity and resolution, ¹⁸F labeled radiotracers for the neuroimaging of σ_1 receptors become more and more important with the increasing number of PET centers.

Considering simple synthesis of ¹⁸F labeled radiotracers via nucleophilic ¹⁸F⁻ substitution of the corresponding tosylate precursor, we have synthesized three fluoro-oligo-ethoxylated 4-benzylpiperazine ligands and measured their affinity for σ_1 receptors by in vitro radioligand binding assays. Moreover, we synthesized [¹⁸F]**6**, determined its log*D* value, and evaluated its potential as a putative PET tracer for imaging of σ_1 receptors by biodistribution studies in mice and ex vivo autoradiography in rat.

2. Results and discussion

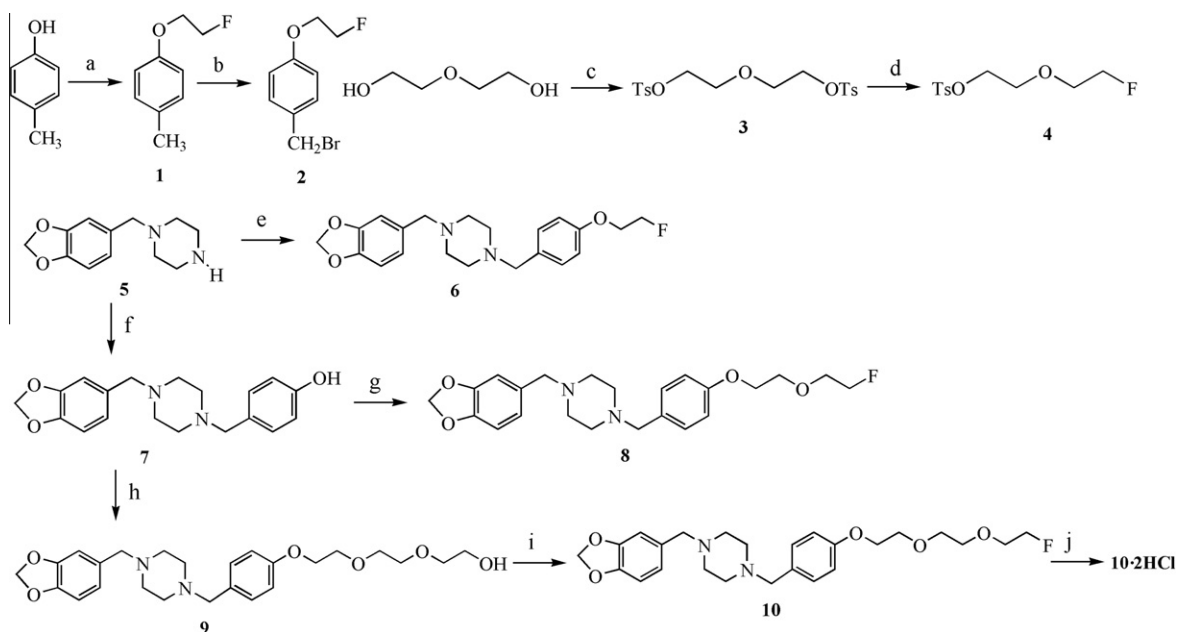
2.1. Chemistry

The synthetic route of fluoro-ethoxylated 4-benzylpiperazine derivatives is shown in Scheme 1. Compound **1** was synthesized according to the method reported in the literature with minor modification.²³ *p*-Cresol reacted with 1-bromo-2-fluoroethane instead of fluoroethyl tosylate to obtain compound **1**. Compound **2**, **3**, **4** were synthesized based on the method reported in the literature.^{23–25} Alkylation of compound **5** with **2** provided compound **6**. Compound **5** reacted with 4-hydroxybenzaldehyde to get compound **7**. Compound **7** reacted with compound **4** or 2-(2-(2-chloroethoxy)ethoxy)ethanol to provide compound **8** or compound **9**, respectively. Fluorination of Compound **9** with DAST (diethylamino sulfur trifluoride) provided Compound **10**, which was recrystallized with the form of salt in methanol. The target compounds (**6**, **8**, and **10**) were characterized by NMR, MS, and EA.

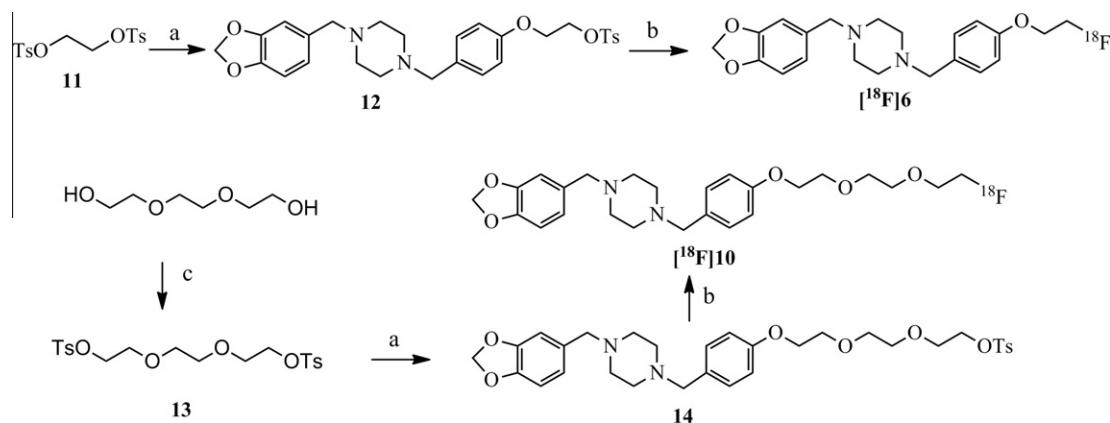
2.2. Radiolabeling

The synthetic route of the tosylate precursors and the corresponding ¹⁸F labeled radiotracers ([¹⁸F]**6** and [¹⁸F]**10**) is given in Scheme 2. Compound **11** and **13** were synthesized according to the method reported in the literature.^{26,27} Compound **7** reacted with compound **11** or **13** to provide the tosylate precursor **12** or **14**, respectively. [¹⁸F]Fluoride was transferred into the Kryptofix 222/potassium carbonate solution, which is made up by Kryptofix 222 and potassium carbonate in acetonitrile/water. After the solvent was removed under a stream of nitrogen at 120 °C and the residue azeotropically dried three times with 1 mL of anhydrous acetonitrile, the tosylate precursor (**12** or **14**) dissolved in anhydrous acetonitrile was added to the reaction tube. The reaction was carried out at 100 °C for 5 min. After cooling to room temperature, the mixture was passed through a Sep-Pak C18 cartridge to remove inorganic salts including [¹⁸F]KF. The crude product was eluted and purified by an isocratic semi-preparative radio-HPLC using a reverse-phase column and mobile phase consisting of acetonitrile and water (containing 10 mM NH₄OAc) (80:20 v/v) at a flow rate of 4 mL/min.

In order to identify the radiotracer, [¹⁸F]**6** and [¹⁸F]**10** were co-injected and co-eluted with the corresponding unlabeled compounds, respectively. Their HPLC profiles using acetonitrile and water (containing 10 mM NH₄OAc) (80:20 v/v) at a flow rate of 1 mL/min are presented in Figure 1. The retention times of unlabeled **6** and [¹⁸F]**6** were observed to be 5.56 min and 5.60 min, respectively. The retention times of unlabeled **10** and [¹⁸F]**10** were observed to be 5.23 min and 5.28 min, respectively. The difference in retention time was in good agreement with the time lag, which corresponds to the volume and flow rate within the distance between the UV and radioactivity detector of our HPLC system. After purification by radio-HPLC, the radiochemical purity of the radioactive products was higher than 99%. The isolated radiochemical yields of [¹⁸F]**6** and [¹⁸F]**10** were 30–50% ($n = 3$) and 20–40% ($n = 3$), respectively. The specific activity of the product was estimated to be 1000 Ci/mmol.



Scheme 1. Synthetic route of fluoro-ethoxylated 4-benzylpiperazine derivatives. Reagents and conditions: (a) 1-bromo-2-fluoroethane, K₂CO₃, acetone, 80 °C, 4 h; (b) NBS, AIBN, CCl₄, 90 °C, 3 h; (c) 4-toluene sulfonyl chloride, KOH, CH₂Cl₂, 0 °C to rt, 10 h; (d) TBAF, acetonitrile, 90 °C, 8 h; (e) **2**, CH₂Cl₂, rt, 60 h; (f) (i) 4-hydroxybenzaldehyde, 1,2-dichloroethane, rt, 2 h; (ii) NaBH(OAc)₃, rt, 12 h; (g) **4**, K₂CO₃, acetonitrile, 90 °C, 14 h; (h) 2-(2-(2-chloroethoxy)ethoxy)ethanol, DMF, K₂CO₃, 100 °C, 11 h; (i) DAST, CHCl₃, –78 °C, 1 h; (j) ethanol, conc. HCl, rt, 1 h.



Scheme 2. Synthetic route of the tosylate precursors and the corresponding ^{18}F labeled radiotracers. Reagents and conditions: (a) **7**, K_2CO_3 , CH_3CN , 90°C , 8 h; (b) $^{18}\text{F}^-$, Kryptofix 222, K_2CO_3 , CH_3CN , 100°C , 5 min; (c) 4-toluene sulfonyl chloride, KOH , CH_2Cl_2 , 0°C to rt, 10 h.

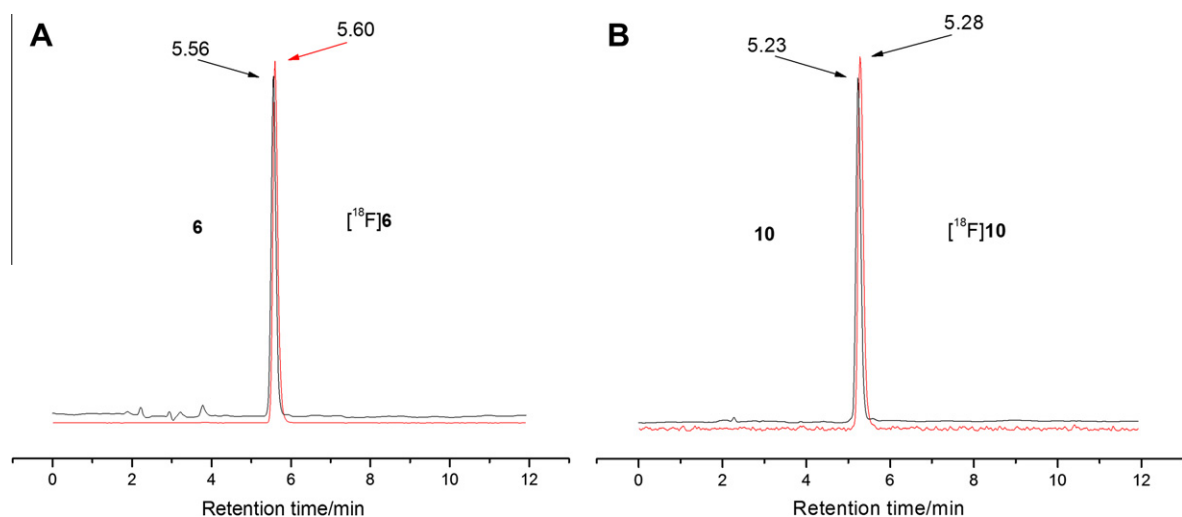


Figure 1. (A) HPLC co-elution profiles of **6** and ^{18}F **6**, with retention time of 5.56 and 5.60 min, respectively. (B) HPLC co-elution profiles of **10** and ^{18}F **10**, with retention time of 5.23 and 5.28 min, respectively.

The apparent distribution coefficients of ^{18}F **6** and ^{18}F **10** were determined in a 1-octanol/ 0.05 mol L^{-1} sodium phosphate buffer system at pH 7.4 as previously reported.²⁸ At pH 7.4, the $\log D$ values of ^{18}F **6** and ^{18}F **10** were determined to be 2.57 ± 0.10 and 2.22 ± 0.06 ($n = 3$), respectively, which are within the range expected to give high brain uptake.

2.3. Biological studies

2.3.1. In vitro radioligand competition studies

σ_1 and σ_2 receptor competition binding assays were performed as previously reported.²⁹ The σ_1 and σ_2 receptor affinities of fluoro-oligo-ethoxylated 4-benzylpiperazine derivatives were determined in competition experiments with the radioligands (+)- ^3H pentazocine (the mean working concentration: 2.0 nM) and ^3H ditolylguanidine (the mean working concentration: 1.7 nM) using rat brain and rat liver preparations, respectively. In vitro competition binding assays showed that **6** exhibited low nanomolar affinity for σ_1 receptors ($K_i = 1.85 \pm 1.59\text{ nM}$, Table 1) and high subtype selectivity (σ_2 receptor: $K_i = 291 \pm 111\text{ nM}$; $K_i(\sigma_2)/K_i(\sigma_1) = 157$, Table 1). Compared to the previously reported BP derivatives, substituent at *para*-position of the benzyl moiety with small steric group, such as F, I or $\text{OCH}_2\text{CH}_2\text{F}$, possessed low nanomolar affinity for σ_1 receptors. Introducing $\text{OCH}_2\text{CH}_2\text{F}$ group led to an increase of

Table 1

Binding affinities of the fluoro-oligo-ethoxylated 4-benzylpiperazine derivatives towards σ_1 and σ_2 receptors^a

Compound	$K_i(\sigma_1)$ (nM)	$K_i(\sigma_2)$ (nM)	$K_i(\sigma_2)/K_i(\sigma_1)$
6	1.85 ± 1.59	291 ± 111	157
8	40.7 ± 22.8	666 ± 106	16.4
10	505 ± 120	1420 ± 160	2.81
BP-F ^b	0.85 ± 0.91	52.2 ± 13.3	61.4
BP-I ^b	0.80 ± 0.14	61.1 ± 20.1	76.4
Haloperidol	4.95 ± 1.74	20.7 ± 0.07	4.18

^a Values are means \pm SD of three experiments performed in triplicate.

^b From Ref. 22.

subtype selectivity. But substitution at the same position with increased length of fluoro-oligo-ethoxylated group led to decreased affinities for σ_1 receptors. With high affinity and high subtype selectivity, compound **6** is a more promising σ_1 receptor ligand compared to BP-F and BP-I.

2.3.2. Biodistribution and blocking studies in mice

In vivo biodistribution studies of ^{18}F **6** and ^{18}F **10** were performed in male ICR mice. The values reflecting the uptake of radiotracer in the organs of interest at 2, 15, 30, 60 and 120 min after intravenous administration of ^{18}F **6** or ^{18}F **10** (0.1 mL,

Table 2
Biodistribution of [¹⁸F]6 in male ICR mice^a

Organ	2 min	15 min	30 min	60 min	120 min
Blood	1.29 ± 0.12	1.05 ± 0.25	0.92 ± 0.07	1.11 ± 0.12	0.88 ± 0.21
Brain	6.00 ± 0.60	6.30 ± 0.32	5.73 ± 0.52	5.23 ± 0.51	4.72 ± 1.28
Heart	10.19 ± 1.63	7.49 ± 1.44	5.42 ± 0.41	2.99 ± 0.22	2.67 ± 0.93
Liver	4.87 ± 1.89	9.73 ± 1.53	7.76 ± 0.78	7.66 ± 1.42	7.19 ± 1.73
Spleen	3.39 ± 1.17	6.13 ± 1.37	5.47 ± 0.39	4.92 ± 0.68	4.38 ± 0.56
Lung	19.97 ± 4.11	11.53 ± 0.91	8.09 ± 2.59	5.77 ± 1.34	4.82 ± 1.26
Kidney	19.26 ± 1.56	12.54 ± 1.23	9.34 ± 0.88	6.13 ± 0.93	4.54 ± 0.72
Muscle	3.27 ± 0.39	4.34 ± 1.11	2.66 ± 0.44	2.05 ± 0.43	2.26 ± 0.72
Stomach ^b	1.00 ± 0.29	1.77 ± 0.38	1.65 ± 0.35	1.97 ± 0.77	1.54 ± 0.80
Small intestine ^b	7.47 ± 0.72	7.94 ± 1.97	8.35 ± 1.29	8.00 ± 1.77	8.57 ± 5.71
Bone	3.05 ± 0.73	5.17 ± 1.32	3.53 ± 0.52	3.20 ± 0.99	3.15 ± 0.58
Brain/blood	4.65	6.00	6.23	4.71	5.36

^a Data are means of %ID/g of tissue ± SD, n = 5.

^b %ID/organ.

4 μCi/0.02 nmol) are summarized in Table 2 and Table 3, respectively. [¹⁸F]6 showed a high initial brain uptake, with slow clearance and high brain-to-blood ratios. The radiotracer concentration determined in the brain was highest at 15 min post-injection (p.i.) with 6.30 ± 0.32%ID/g, and slowly cleared thereafter with 5.73 ± 0.52%ID/g at 30 min, 5.23 ± 0.51%ID/g at 60 min, and 4.72 ± 1.28%ID/g at 120 min p.i. The values were higher than that of [¹¹C]SA4503³⁰ and [¹⁸F]fluspidine.²¹ In contrast to the high uptake and retention in the brain, the blood radiotracer levels were low with 1.05 ± 0.25%ID/g at 15 min and 0.88 ± 0.21%ID/g at 120 min p.i., resulting in high brain-to-blood ratios (6.00, 6.23, 4.71, and 5.36 at 15, 30, 60, and 120 min p.i., respectively). Similar to what was found for [¹⁸F]fluspidine, high uptakes (6.13–12.54%ID/g at 15 min p.i.) were observed in organs known to contain σ receptors, including the lungs, kidneys, heart, spleen and liver, followed by slow clearance over time. Different to what was found for [¹⁸F]6, [¹⁸F]10 showed a high initial brain uptake, with fast washout and low brain-to-blood ratios. Fast washout of radiotracer was also observed in the organs known to contain σ receptors, which was in good agreement with low affinity of [¹⁸F]10 for σ₁ receptors. In addition, the accumulation of radiotracer in the bone at 120 min p.i. was quite low suggesting that both [¹⁸F]6 and [¹⁸F]10 were relatively stable to in vivo defluorination.

In order to verify the specific binding of [¹⁸F]6 to σ receptors in vivo, the effects of preinjection of haloperidol (0.1 mL, 1.0 mg/kg) on the biodistribution of radioactivity in various organs of male ICR mice were examined. Either saline or haloperidol was injected 5 min prior to the radiotracer injection. The results of blocking studies at 60 min p.i. are given in Table 4. Of particular interest was a significant reduction by 71% (*p* < 0.001) of the

Table 3
Biodistribution of [¹⁸F]10 in male ICR mice^a

Organ	2 min	15 min	30 min	60 min	120 min
Blood	3.63 ± 1.00	3.42 ± 1.13	2.53 ± 0.55	1.82 ± 0.88	1.15 ± 0.18
Brain	6.42 ± 0.82	1.66 ± 0.21	0.97 ± 0.20	0.84 ± 0.12	0.77 ± 0.18
Heart	6.75 ± 1.37	2.63 ± 0.51	1.67 ± 0.40	1.26 ± 0.22	1.01 ± 0.12
Liver	4.98 ± 0.90	3.90 ± 0.53	2.84 ± 0.47	2.27 ± 0.25	1.52 ± 0.20
Spleen	5.95 ± 1.17	6.54 ± 1.07	2.93 ± 0.88	1.18 ± 0.20	0.78 ± 0.29
Lung	15.30 ± 1.94	4.01 ± 0.34	2.55 ± 0.52	1.55 ± 0.22	0.90 ± 0.17
Kidney	27.41 ± 2.43	14.39 ± 1.47	6.52 ± 1.27	3.91 ± 0.48	2.35 ± 0.49
Muscle	4.18 ± 0.46	2.39 ± 0.32	1.09 ± 0.44	0.98 ± 0.15	1.02 ± 0.32
Stomach ^b	2.94 ± 1.20	2.53 ± 0.69	0.97 ± 0.40	1.05 ± 0.19	0.95 ± 0.13
Small intestine ^b	7.54 ± 2.33	7.57 ± 1.29	6.63 ± 1.43	5.65 ± 2.66	2.07 ± 0.28
Bone	3.08 ± 0.32	2.89 ± 0.64	1.80 ± 0.57	1.35 ± 0.26	1.89 ± 0.72
Brain/blood	1.77	0.49	0.38	0.46	0.67

^a Data are means of %ID/g of tissue ± SD, n = 5.

^b %ID/organ.

accumulation of radiotracer in the brain at 60 min p.i. which corresponded to values obtained with [¹⁸F]fluspidine.²¹ Moreover, the concentration of radiotracer in organs known to possess σ₁ receptors was significantly reduced with values of 47% determined in heart, 52% in spleen, and 58% in lung. These data suggested that the binding of [¹⁸F]6 to σ₁ receptors was specific in vivo. The same blocking studies of [¹⁸F]10 was carried out for comparison (Table 5). No reduction of radiotracer accumulation in the above-mentioned organs known to contain σ₁ receptors was found, which was in accord with low affinity of [¹⁸F]10 for σ₁ receptors.

2.3.3. Ex vivo autoradiography

In order to investigate the radiotracer accumulation in different brain regions, brain sections were evaluated by ex vivo autoradiography at 60 min p.i. of [¹⁸F]6 (350 μCi/2 nmol) in rat (Fig. 2). The ex vivo autoradiography in rat brain showed high accumulation of radiotracer in the brain areas known to possess high expression of σ₁ receptors. For example, high accumulation of radiotracer was found in brain areas such as facial nucleus, cerebellum, cortex, midbrain, hypothalamus, and hippocampus. Moderate accumulation of radiotracer was found in the thalamus. Comparably low accumulation of radiotracer was found in the striatum, nucleus accumbens and olfactory bulb.

In order to confirm the specific binding of [¹⁸F]6 to σ₁ receptors ex vivo, the effects of preinjection of haloperidol (0.2 mL, 1.0 mg/kg) on the accumulation of radiotracer in the brain areas of male SD rat were investigated. Administration of haloperidol 5 min prior to injection of [¹⁸F]6 significantly reduced the concentration of radiotracer in the above-mentioned areas known to possess high expression of σ₁ receptors. Therefore, the high radioactive signals in corresponding distribution of σ₁ receptors are specific.

Currently, in vivo [¹¹C]SA4503 imaging studies have shown that the density of σ₁ receptors was decreased in Parkinson's disease (PD) and Alzheimer's disease (AD) patients.^{10,11} This tracer could be used as a probe of clinical studies in σ₁ receptors imaging in the above brain diseases. However, use of [¹¹C]SA4503 needs an on-site cyclotron. Longer half-life ¹⁸F labelled ligand is more suitable for σ₁ receptors imaging. Unfortunately, there is lack of suitable ¹⁸F-labelled PET radiotracers for the neuroimaging of σ₁ receptors until now. The major problems of [¹⁸F]FPS, the only ¹⁸F labeled σ₁ receptor radiotracer investigated in human studies, are the irreversible kinetics and no suitable reference regions.¹⁴ In our previous work, based on the proposal that the possible mechanisms of the treatment effect of sodium channel mediated disease of BP-Br could be related to σ₁ receptors, we found that BP derivatives possessed high affinity for σ₁ receptors. [¹²⁵I]BP-I showed specific binding to σ₁ receptors in vivo.²² Considering

Table 4
Effects of preinjection of haloperidol (0.1 mL, 1.0 mg/kg) 5 min prior to the injection of [¹⁸F]**6** on the biodistribution of radioactivity in male ICR mice^a

Organ	60 min (Control)	60 min (Blocking)	% Blocking	<i>p</i> ^b
Blood	0.93 ± 0.11	1.85 ± 0.23	99	<0.001
Brain	5.44 ± 0.58	1.59 ± 0.19	−71	<0.001
Heart	3.29 ± 0.41	1.74 ± 0.15	−47	<0.001
Liver	7.39 ± 1.25	3.56 ± 0.77	−52	<0.001
Spleen	5.32 ± 0.40	2.55 ± 0.23	−52	<0.001
Lung	5.04 ± 0.61	2.14 ± 0.17	−58	<0.001
Kidney	6.67 ± 0.67	3.83 ± 0.67	−43	<0.001
Muscle	2.50 ± 0.29	1.50 ± 0.13	−40	<0.001
Stomach ^c	1.33 ± 0.17	2.49 ± 0.87	87	0.019
Small intestine ^c	8.05 ± 2.41	7.02 ± 2.20	−13	0.533
bone	2.80 ± 0.13	2.93 ± 0.56	5	0.625

^a Data are means of %ID/g of tissue ± SD, *n* = 4–5.

^b *p* values for the control versus blocking group at 60 min p.i. calculated by Student's *t* test (independent, two-tailed).

^c %ID/organ.

Table 5
Effects of preinjection of haloperidol (0.1 mL, 1.0 mg/kg) 5 min prior to the injection of [¹⁸F]**10** on the biodistribution of radioactivity in male ICR mice^a

Organ	60 min (Control)	60 min (Blocking)	% Blocking	<i>p</i> ^b
Blood	1.25 ± 0.11	2.16 ± 0.31	73	<0.001
Brain	0.75 ± 0.12	1.13 ± 0.13	51	0.001
Heart	1.22 ± 0.26	1.62 ± 0.34	33	0.072
Liver	2.01 ± 0.17	2.57 ± 0.24	28	0.004
Spleen	0.95 ± 0.39	1.51 ± 0.28	59	0.032
Lung	1.07 ± 0.15	1.87 ± 0.23	75	<0.001
Kidney	3.22 ± 0.76	3.60 ± 0.55	12	0.385
Muscle	0.90 ± 0.18	1.39 ± 0.38	54	0.029
Stomach ^c	1.08 ± 0.43	1.17 ± 0.34	8	0.730
Small intestine ^c	5.01 ± 1.74	7.57 ± 1.69	51	0.062
Bone	1.17 ± 0.39	1.60 ± 0.24	37	0.091

^a Data are means of %ID/g of tissue ± SD, *n* = 4–5.

^b *p* values for the control versus blocking group at 60 min p.i. calculated by Student's *t* test (independent, two-tailed).

^c %ID/organ.

higher detection sensitivity and resolution of imaging with PET than that with SPECT, and simple synthesis of ¹⁸F labeled radiotracers via nucleophilic ¹⁸F[−] substitution of the corresponding tosylate precursor, we synthesized and evaluated fluoro-oligo-ethoxylated 4-benzylpiperazine ligands for σ_1 receptors. It is encouraging that compound **6** exhibited low nanomolar affinity for σ_1 receptors and higher subtype selectivity than BP-I (Table 1). Generally speaking, proper lipophilicity of receptor ligand may be responsible for high brain uptake and low non-specific binding. The lipophilicity of [¹⁸F]**6** ($\log D_{pH\ 7.4} = 2.57$), which is lower than that of [¹²⁵I]BP-I ($\log D_{pH\ 7.4} = 2.98$), is appropriate for a σ_1 receptor ligand. The radiotracer concentration determined in the brain after intravenous administration of [¹⁸F]**6** is higher than that of [¹²⁵I]BP-I. The brain uptake is also higher than that of [¹¹C]SA4503³⁰ and [¹⁸F]fluspidine.²¹ In addition, the percentage of specific uptake in the brain was 71% (60 min p.i.), which is comparable to that determined for [¹¹C]SA4503 (about 70%),³⁰ and higher than that of [¹²⁵I]BP-I (63%)²² and [¹⁸F]fluspidine (62%).²¹ Third, the ex vivo autoradiography at 1 h after intravenous injection of [¹⁸F]**6** in rat showed a high accumulation of radiotracer in brain areas known to possess high expression of σ_1 receptors such as the facial nucleus, cerebellum, cortex, midbrain, hypothalamus, and hippocampus. Administration of haloperidol 5 min prior to injection of [¹⁸F]**6** significantly reduced the concentration of radiotracer in the above-

mentioned areas, which confirmed that the high radioactive signals to the corresponding distribution of σ_1 receptors are specific. Therefore, the encouraging results including high affinity and selectivity towards σ_1 receptors, high brain uptake and specific binding, as well as limited in vivo defluorination, warrant further evaluation of [¹⁸F]**6** as a putative tracer for imaging σ_1 receptors with PET.

As indicated in Introduction, many σ receptor ligands have affinity for the VACHT and the EBP.^{15–18} Although SA4503 was reported to show affinities for VACHT¹⁵ and EBP,¹⁶ [¹¹C]SA4503 did not seem to bind to VACHT¹⁹ and EBP²⁰ in the rat brain in vivo. Moreover, selectivity to the other neuroreceptors should be taken into consideration when designing new selective ligands. For example, Kawamura et al have demonstrated σ_1 receptor selectivity of [¹¹C]SA4503 by treating with the other receptors selective ligands.³⁰ For σ_1 receptor radiotracer applications in human brain, appropriate brain kinetics and peripheral metabolism should also be considered. The investigations including the selectivity to the other neuroreceptors as well as the brain kinetics and peripheral metabolism of [¹⁸F]**6** are in progress.

3. Conclusions

Fluoro-oligo-ethoxylated 4-benzylpiperazine derivative **6** has been synthesized and evaluated as σ_1 receptor ligand with high affinity and high subtype selectivity. [¹⁸F]**6** has been obtained with high radiochemical purity. The $\log D$ value of [¹⁸F]**6** was within the range expected to give excellent brain uptake. In biodistribution studies [¹⁸F]**6** was found to possess very high initial brain uptake followed by slow clearance. The in vivo binding pattern of the tracer was in good agreement with the known distribution of σ_1 receptors, and blocking studies confirmed high specific binding. The ex vivo autoradiography in rat brain showed high accumulation of radiotracer in the brain areas known to possess high expression of σ_1 receptors. These findings suggest further evaluation of [¹⁸F]**6** as a suitable radiotracer for imaging σ_1 receptors with PET in vivo.

4. Experimental section

4.1. General information

All reagents and chemicals were purchased from commercial suppliers and used without further purification unless otherwise stated. Thin layer chromatography (TLC): Silica gel 60 F254 plates (Merck). Flash column chromatography was conducted using silica gel [45–75 μ m]. The mobile phase used is reported in the experimental procedure for each compound. Melting point was recorded on a SGW X-4 micro melting point apparatus (Shanghai precision scientific instrument Co., LTD, China) and was uncorrected. ¹H NMR spectra were recorded on a Bruker Avance III (400 MHz) NMR spectrometer. Chemical shift (δ) are reported in ppm downfield from tetramethylsilane and coupling constants (*J*) are reported in Hertz (Hz). ¹³C NMR spectra were recorded on a Bruker Avance III (100 MHz) NMR spectrometer. MS spectra were obtained by Quattro micro API ESI/MS (Waters, USA). Elemental analyses (C, H, N) were obtained on an Elementar 240C (Perkin Elmer, USA).

HPLC analyses were performed on a Waters 600 system (Waters corporation, USA) equipped with Waters 2489 UV–VIS detector, and Raytest Gabi NaI(Tl) scintillation detector (Raytest, Germany). The sample was analyzed on a Agela Venusil MP C18 column (250 mm × 4.6 mm, 5 μ m) using acetonitrile and water (containing 10 mM NH₄OAc) (80:20 v/v) as mobile phase at a flow rate of 1 mL/min. HPLC separation was carried out on a Shimadzu SCL-

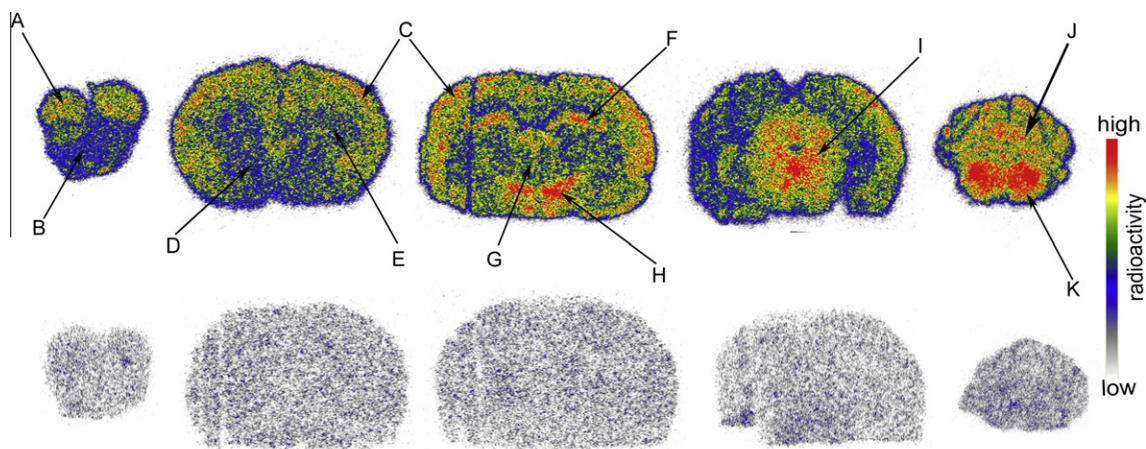


Figure 2. Ex vivo autoradiograms of the rat coronal brain sections at 1 h after intravenous injection of [^{18}F]6. (A) frontal cortex; (B) olfactory bulb; (C) cerebral cortex; (D) nucleus accumbens; (E) striatum; (F) hippocampus; (G) thalamus; (H) hypothalamus; (I) midbrain; (J) cerebellum; (K) facial nucleus.

20 AVP HPLC system (Shimadzu Corporation, Japan) equipped with a SPD-M20A UV–VIS detector operating at a wavelength of 254 nm, and a Bioscan Flow Count 3200 NaI/PMT γ -radiation scintillation detector. The sample was separated on a Grace Allsphere ODS-2 column (250 mm \times 10 mm, 5 μm) using acetonitrile and water (containing 10 mM NH_4OAc) (80:20 v/v) as mobile phase at a flow rate of 4 mL/min.

Male ICR mice (5 weeks, 18–22 g) and male Sprague-Dawley rats (9 weeks, 220 g) were purchased from Peking University Health Science Center. All procedures of the animal experiments were performed in compliance with relevant laws and institutional guidelines. All of the animal experiments were approved by the Institutional Animal Care and Use Committee of Beijing Normal University.

4.2. 1-(1,3-Benzodioxol-5-ylmethyl)-4-(4-(2-fluoroethoxy)benzyl)piperazine (6)

1-Piperonylpiperazine (**5**, 35.0 mg, 0.16 mmol) was dissolved in anhydrous CH_2Cl_2 (2 mL). Compound **2** (44.5 mg, 0.18 mmol) was then added with stirring for over 60 h at room temperature. The reaction mixture was concentrated under vacuum and purified by silica gel column chromatography using ethyl acetate/petroleum ether/triethylamine (1/4/0.1, v/v/v) as the mobile phase to afford **6** as a white solid (23.5 mg, 35%). ^1H NMR (400 MHz, CDCl_3) δ (ppm): 7.23 (d, $J = 8.4$ Hz, 2H), 6.87 (d, $J = 8.6$ Hz, 2H), 6.84 (s, 1H), 6.73 (s, 2H), 5.93 (s, 2H), 4.80 (t, $J = 4.2$ Hz, 1H), 4.69 (t, $J = 4.2$ Hz, 1H), 4.23 (t, $J = 4.2$ Hz, 1H), 4.16 (t, $J = 4.2$ Hz, 1H), 3.46 (s, 2H), 3.42 (s, 2H), 2.46 (br s, 8H). ^{13}C NMR (100 MHz, CDCl_3) δ (ppm) 52.97, 62.37, 62.75, 67.04, 67.25, 81.10, 82.80, 100.83, 100.88, 107.81, 109.54, 114.34, 122.22, 130.44, 130.87, 132.13, 146.53, 147.58, 157.54. ESI-MS, $[\text{M}+\text{H}]^+$ ($m/z = 372.7$). Mp: 98.4–99.6 $^\circ\text{C}$. Anal. Calcd for $\text{C}_{21}\text{H}_{25}\text{FN}_2\text{O}_3$: C 67.72, H 6.77, N 7.52. Found: C 67.63, H 6.875, N 7.215.

4.3. 1-(1,3-Benzodioxol-5-ylmethyl)-4-(4-hydroxybenzyl)piperazine (7)

1-Piperonylpiperazine (**5**, 521.2 mg, 2.37 mmol) was dissolved in 1,2-dichloroethane (15 mL), and 4-hydroxybenzaldehyde (323.5 mg, 2.65 mmol) was added with stirring for 2 h at room temperature. Then $\text{NaBH}(\text{OAc})_3$ (821.9 mg, 3.88 mmol) was added into the reaction. This reaction mixture was stirred at room temperature overnight. The mixture was washed with saturated NaHCO_3 and concentrated under vacuum. The aqueous phase was

extracted with CH_2Cl_2 (20 mL \times 3). The combined organic phases were dried over Na_2SO_4 and concentrated under vacuum. The crude product was purified by silica gel column chromatography using ethyl acetate/petroleum ether (1/1, v/v) as the mobile phase to afford **7** (Registry Number: 757195-64-5) as a white solid (464.7 mg, 75%). ESI-MS, $[\text{M}+\text{H}]^+$ ($m/z = 327.4$).

4.4. 1-(1,3-Benzodioxol-5-ylmethyl)-4-(4-(2-(2-fluoroethoxy)ethoxy)benzyl)piperazine (8)

A mixture of **4** (58.1 mg, 0.22 mmol), **7** (92.0 mg, 0.28 mmol), K_2CO_3 (30.61 mg, 0.22 mmol) and acetonitrile (5 mL) was heated to 90 $^\circ\text{C}$ with stirring for 14 h. Then the reaction mixture was concentrated under vacuum and the crude product was dissolved in CH_2Cl_2 (50 mL) and washed with water (50 mL). The organic layer was dried over MgSO_4 and concentrated under vacuum and purified by silica gel column chromatography using ethyl acetate/petroleum ether/triethylamine (1/2/0.1, v/v/v) as the mobile phase to afford **8** as a white solid (51.7 mg, 56%). ^1H NMR (400 MHz, CDCl_3) δ (ppm): 7.20 (d, $J = 8.5$ Hz, 2H), 6.86 (d, $J = 8.5$ Hz, 2H), 6.84 (s, 1H), 6.73 (s, 2H), 5.93 (s, 2H), 4.65 (t, $J = 4.1$ Hz, 1H), 4.53 (t, $J = 4.1$ Hz, 1H), 4.13 (t, $J = 4.8$ Hz, 2H), 3.88 (t, $J = 4.8$ Hz, 2H), 3.86 (t, $J = 4.3$ Hz, 1H), 3.78 (t, $J = 4.1$ Hz, 1H), 3.45 (s, 2H), 3.41 (s, 2H), 2.45 (br s, 8H). ^{13}C NMR (100 MHz, CDCl_3) δ (ppm): 52.83, 52.89, 62.34, 62.70, 67.52, 69.98, 70.49, 70.69, 82.32, 84.00, 100.85, 107.83, 109.56, 114.37, 122.27, 130.25, 130.44, 131.99, 146.59, 147.61, 157.91. ESI-MS, $[\text{M}+\text{H}]^+$ ($m/z = 417.1$). Mp: 80–81 $^\circ\text{C}$. Anal. Calcd for $\text{C}_{23}\text{H}_{29}\text{FN}_2\text{O}_4$: C 66.33, H 7.02, N 6.73. Found: C 66.04, H 6.428, N 6.529.

4.5. 1-(1,3-Benzodioxol-5-ylmethyl)-4-(4-(2-(2-(2-hydroxyethoxy)ethoxy)ethoxy)benzyl)piperazine (9)

Compound **7** (542.3 mg, 1.66 mmol) was dissolved in DMF (6 mL), 2-(2-(2-chloroethoxy)ethoxy)ethanol (243 μL , 1.99 mmol) and K_2CO_3 (688.9 mg, 4.98 mmol) were added. The reaction mixture was heated to 100 $^\circ\text{C}$ with stirring for 11 h. Then the mixture was concentrated under vacuum. The crude product was then dissolved in CHCl_3 (30 mL), washed with water (30 mL), dried over Na_2SO_4 , and purified by silica gel column chromatography using ethyl acetate/petroleum ether (1/1, v/v) as the mobile phase to afford **9** (280.0 mg, 37%). ^1H NMR (400 MHz, CDCl_3) δ (ppm): 7.20 (d, $J = 8.5$ Hz, 2H), 6.85 (d, $J = 8.6$ Hz, 2H), 6.84 (s, 1H), 6.73 (s, 2H), 5.93 (s, 2H), 4.12 (t, $J = 4.8$ Hz, 2H), 3.86 (t, $J = 4.8$ Hz, 2H), 3.73–3.69 (m, 6H), 3.63–3.60 (m, 2H), 3.46 (s, 2H), 3.42 (s, 2H), 2.46 (br s, 8H).

4.6. 1-(1,3-Benzodioxol-5-ylmethyl)-4-(4-(2-(2-(2-fluoroethoxy)ethoxy)ethoxy)benzyl)piperazine (10)

Compound **9** (230.0 mg, 0.50 mmol) was dissolved in anhydrous CHCl_3 (5 mL). DAST (132.5 μL) was slowly added at -78°C . The mixture was stirring at -78°C for 1 h and then at room temperature for 4 h. Saturated NaHSO_3 was added and was stirring for 30 min. The aqueous phase was extracted with CHCl_3 (20 mL \times 3). The combined organic phases were dried over MgSO_4 and concentrated under vacuum. The crude product was purified by silica gel column chromatography using ethyl acetate/petroleum ether/triethylamine (1/2/0.1, v/v/v) as the mobile phase to afford **10** as a colorless oil (130.0 mg, 56%). Then the oil was dissolved in ethanol (2 mL), concentrated hydrochloric acid was added and the mixture was stirring for 1 h. The product was filtered and recrystallized in methanol to afford **10**·2HCl as a white crystal. ^1H NMR (400 MHz, CDCl_3) δ (ppm): 7.20 (d, $J = 8.4$ Hz, 2H), 6.86 (s, 1H), 6.84 (s, 2H), 6.73 (s, 2H), 5.92 (s, 2H), 4.62 (t, $J = 4.2$ Hz, 1H), 4.50 (t, $J = 4.2$ Hz, 1H), 4.12 (t, $J = 4.9$ Hz, 2H), 3.85 (t, $J = 4.9$ Hz, 2H), 3.80 (t, $J = 4.2$ Hz, 1H), 3.74–3.71 (m, 5H), 3.45 (s, 2H), 3.42 (s, 2H), 2.46 (br s, 8H). ^{13}C NMR (100 MHz, CDCl_3) δ (ppm): 52.89, 62.36, 62.72, 67.46, 69.85, 70.36, 70.56, 70.87, 82.30, 83.98, 100.84, 107.81, 109.57, 114.32, 122.24, 130.26, 130.39, 132.06, 146.55, 147.59, 157.94. ESI-MS, $[\text{M}+\text{H}]^+$ ($m/z = 461.5$). Anal. Calcd for $\text{C}_{25}\text{H}_{35}\text{Cl}_2\text{FN}_2\text{O}_5$: C 56.29, H 6.61, N 5.25. Found: C 56.34, H 6.696, N 4.795.

4.7. 1-(1,3-Benzodioxol-5-ylmethyl)-4-(4-(2-(4-methylbenzenesulfonyloxy)ethoxy)benzyl)piperazine (12)

A mixture of **11** (1.04 g, 2.81 mmol), compound **7** (305.5 mg, 0.94 mmol), K_2CO_3 (132.8 mg, 0.96 mmol), and CH_3CN (6 mL) was heated to reflux for 8 h. The mixture was concentrated under vacuum and the residue was dissolved in CH_2Cl_2 , washed with water, dried over MgSO_4 and concentrated under vacuum. The crude product was purified by silica gel column chromatography and recrystallized in ethanol to afford **12** (199.7 mg, 41%) as a white crystal. ^1H NMR (400 MHz, CDCl_3) δ (ppm): 7.82 (d, $J = 8.3$ Hz, 2H), 7.34 (d, $J = 8.1$ Hz, 2H), 7.19 (d, $J = 7.7$ Hz, 2H), 6.84 (s, 1H), 6.73 (s, 3H), 6.71 (s, 1H), 5.93 (s, 2H), 4.36 (t, $J = 4.8$ Hz, 2H), 4.13 (t, $J = 4.8$ Hz, 2H), 3.44 (s, 2H), 3.42 (s, 2H), 2.45 (br s, 11H). ESI-MS, $[\text{M}+\text{H}]^+$ ($m/z = 525.2$). Mp: 95.2–96.6 $^\circ\text{C}$.

4.8. 1-(1,3-Benzodioxol-5-ylmethyl)-4-(4-(2-(2-(2-(4-methylbenzenesulfonyloxy)ethoxy)ethoxy)ethoxy)benzyl)piperazine (14)

A mixture of **13** (422.8 mg, 0.92 mmol), compound **7** (100.3 mg, 0.31 mmol), K_2CO_3 (51.3 mg, 0.37 mmol), and CH_3CN (10 mL) was heated to 90°C with stirring for 8 h. The mixture was concentrated under vacuum and the residue was dissolved in CH_2Cl_2 , washed with water, dried over MgSO_4 and concentrated under vacuum. The crude product was purified by silica gel column chromatography using ethyl acetate/petroleum ether/triethylamine (1/1/0.1, v/v/v) as the mobile phase to afford **14** as a colorless oil (83.9 mg, 43%). ^1H NMR (400 MHz, CDCl_3) δ (ppm): 7.79 (d, $J = 8.2$ Hz, 2H), 7.32 (d, $J = 8.1$ Hz, 2H), 7.20 (d, $J = 8.5$ Hz, 2H), 6.84 (d, $J = 6.4$ Hz, 2H), 6.83 (s, 1H), 6.73 (s, 2H), 5.93 (s, 2H), 4.16 (t, $J = 4.8$ Hz, 2H), 4.09 (t, $J = 4.8$ Hz, 2H), 3.81 (t, $J = 4.8$ Hz, 2H), 3.69 (t, $J = 4.8$ Hz, 2H), 3.67–3.64 (m, 2H), 3.62–3.60 (m, 2H), 3.44 (s, 2H), 3.41 (s, 2H), 2.45–2.43 (m, 11H). ESI-MS, $[\text{M}+\text{H}]^+$ ($m/z = 613.2$).

4.9. Radiosynthesis of $[\text{18F}]\text{6}$ and $[\text{18F}]\text{10}$

$[\text{18F}]\text{Fluoride}$ was produced by the Sumitomo cyclotron HM-20PS at Nuclear Medicine Department, Chinese PLA General Hospi-

tal, using $^{18}\text{O}(\text{p,n})^{18}\text{F}$ reaction. The radioactivity was collected on the QMA cartridge (Waters) and the cartridge dried by airflow. The ^{18}F activity was then eluted using 1 mL of a Kryptofix 222/potassium carbonate solution, which is made up of a mixture of 13 mg Kryptofix 222 and 1.1 mg potassium carbonate in acetonitrile/water (0.8 mL/0.2 mL). The solvent was removed under a stream of nitrogen at 120°C and the residue azeotropically dried three times with 1 mL of anhydrous acetonitrile at 120°C , followed by adding 1 mL of the tosylate precursor **12** solution (1 mg/mL) in anhydrous acetonitrile. The reaction mixture was kept at 100°C for 5 min.

After cooling to room temperature, the mixture was passed through a Sep-Pak C18 cartridge previously washed with 10 mL ethanol and 10 mL water. After elution with 10 mL water, inorganic salts including $[\text{18F}]\text{KF}$ was separated from the product. The crude product was recovered into a sample vial by slowly flushing the cartridge with 2 mL of acetonitrile. The solvent was evaporated by N_2 and the residue was purified by an isocratic semi-preparative radio-HPLC (Shimadzu SCL-20 AVP HPLC system, Grace Allsphere ODS-2, 5 μm , 250×10 mm; eluent: 80% CH_3CN and 20% water (containing 10 mM NH_4OAc); flow: 4 mL/min). In order to identify the radioactive product, the unlabeled **6** was co-injected and co-eluted with the radioactive product (Waters 600 HPLC system, Agela Venusil MP C18, 5 μm , $250 \text{ mm} \times 4.6$ mm; eluent: 80% CH_3CN and 20% water (containing 10 mM NH_4OAc); flow: 1 mL/min). To prepare a suitable solution of $[\text{18F}]\text{6}$, the eluted peak corresponding to $[\text{18F}]\text{6}$ was collected, followed by removing of the solvent. Solutions of $[\text{18F}]\text{6}$ in sterile saline containing no more than 8% ethanol were used for animal studies. The same procedures were applied to the synthesis, separation and identification of $[\text{18F}]\text{10}$.

4.10. Determination of logD value

The logD values of $[\text{18F}]\text{6}$ and $[\text{18F}]\text{10}$ were determined by measuring the distribution of the radiotracer in a 1-octanol/0.05 mol L^{-1} sodium phosphate buffer system at pH 7.4. The two phases were pre-saturated with each other. 1-octanol (3 mL) and phosphate buffer (3 mL) were pipetted into a 10 mL plastic centrifuge tube. 100 μL of a solution of HPLC-purified $[\text{18F}]\text{6}$ (20 μCi) or $[\text{18F}]\text{10}$ in ethanol was then added. The tube was vortexed for 5 min, followed by centrifugation for 5 min (3500 rpm, Anke TDL80-2B, China). About 50 μL of the 1-octanol layer was weighed in a tared tube. The 1-octanol layer was removed and about 500 μL of the buffer layer was weighed in a second tared tube. After adding 0.50 mL buffer to the 1-octanol fraction and 0.05 mL of 1-octanol to the aqueous fraction, activity in both tubes was measured in an automatic γ -counter (Wallac 1470 Wizard, USA). Accurate volumes of each counted phase were determined by weight and known densities. The distribution coefficient was determined by calculating the ratio of cpm/mL of 1-octanol layer to that of buffer layer and expressed as logD. Samples from the 1-octanol layer were re-distributed until consistent distribution coefficient values were obtained. The measurement was carried out in triplicate and repeated three times.

4.11. In vitro radioligand competition studies

σ_1 and σ_2 receptor competition binding assays were performed as previously reported.²⁹ Briefly, the σ_1 receptor assay was performed using a rat brain membrane preparation as receptor material and (+)- $[\text{3H}]\text{pentazocine}$ (mean working concentration: 2.0 nM) as radioligand. The σ_2 receptor affinity was determined using rat liver membrane preparation with the radioligand $[\text{3H}]\text{ditolylguanidine}$ (mean working concentration: 1.7 nM) in the presence of 10 μM dextrallorphan to mask σ_1 binding sites.

Nonspecific binding was determined with 10 μM haloperidol. K_i values were calculated according to Cheng and Prusoff and represent data from at least three independent experiments, each performed in triplicate. The results are given as mean \pm standard deviation (SD).

4.12. Biodistribution and blocking studies in mice

Experiments in male ICR mice ($n = 5$, 5 weeks, 18–22 g) were carried out in compliance with the national laws related to the care and experiments on laboratory animals. The HPLC-purified [^{18}F]6 or [^{18}F]10 was injected via tail vein (0.1 mL, 4 $\mu\text{Ci}/0.02$ nmol). The mice were sacrificed by decapitation at various time points. Samples of blood and organs of interest were removed, weighed and counted in an automatic γ -counter (Wallac 1470 Wizard, USA). The results were expressed in terms of the percentage of the injected dose per gram (%ID/g) of blood or organs.

For blocking studies, mice were injected via tail vein with either saline (0.1 mL) or haloperidol (0.1 mL, 1.0 mg/kg) 5 min prior to radiotracer injection. The animals were sacrificed by decapitation at 60 min p.i. Blood or organs were isolated and analyzed as described above for the biodistribution study. Significant differences between control and test groups were determined by Student's t test (independent, two-tailed). The criterion for significance was $p \leq 0.05$.

4.13. Ex vivo autoradiography

Ex vivo autoradiography of the brain was carried out in male Sprague-Dawley rats (9 weeks, 220 g), because of the large size of the brain. The radioligand [^{18}F]6 (350 $\mu\text{Ci}/2$ nmol, 0.2 mL) was intravenously injected into conscious rat via tail vein. For blocking study, another conscious rat was injected with haloperidol (0.2 mL, 1.0 mg/kg) 5 min prior to radiotracer injection. The rat was killed by cervical dislocation 1 h after injection of the radioligand. The brain was rapidly dissected, frozen, and coronally cut into 20 μm thick sections using a cryotome (CM1900, Leica, Germany). The brain sections were dried at room temperature and were exposed to a phosphor plate (PerkinElmer, USA) for 2 h. Ex vivo autoradiographic images were obtained using a phosphor imaging system (Cyclone[®]Plus, PerkinElmer, USA).

Acknowledgments

This work was supported by the National Natural Science Foundation of China (No. 21071023), the Fundamental Research Funds for the Central Universities, and Deutsche Forschungsgemeinschaft (STE 601/10-3).

References and notes

- Hayashi, T.; Su, T.-P. *Cell* **2007**, *131*, 596.
- Katz, J. L.; Su, T.-P.; Hiranita, T.; Hayashi, T.; Tanda, G.; Kopajtic, T.; Tsai, S. Y. *Pharmaceuticals* **2011**, *4*, 880.
- Hayashi, T.; Tsai, S. Y.; Mori, T.; Fujimoto, M.; Su, T.-P. *Expert Opin. Ther. Targets* **2011**, *15*, 557.
- Tsai, S. Y.; Hayashi, T.; Harvey, B. K.; Wang, Y.; Wu, W. W.; Shen, R. F.; Zhang, Y.; Becker, K. G.; Hoffer, B. J.; Su, T.-P. *Proc. Natl. Acad. Sci. U.S.A.* **2009**, *106*, 22468.
- Yi, T. S.; Kyle, R. R.; Ping, S. T. *Synapse (N. Y., NY)* **2012**, *66*, 42.
- Maurice, T.; Su, T. P. *Pharmacol. Ther.* **2009**, *124*, 195.
- Bourrie, B.; Bribe, E.; Derocq, J. M.; Vidal, H.; Casellas, P. *Curr. Opin. Investig. Drugs* **2004**, *5*, 1158.
- Megalizzi, V.; Le Mercier, M.; Decaestecker, C. *Med. Res. Rev.* **2012**, *32*, 410.
- Ito, K.; Hirooka, Y.; Matsukawa, R.; Nakano, M. *Cardiovasc. Res.* **2012**, *93*, 33.
- Mishina, M.; Ishiwata, K.; Ishii, K.; Kitamura, S.; Kimura, Y.; Kawamura, K.; Oda, K.; Sasaki, T.; Sakayori, O.; Hamamoto, M.; Kobayashi, S.; Katayama, Y. *Acta Neurol. Scand.* **2005**, *112*, 103.
- Mishina, M.; Ohyama, M.; Ishii, K.; Kitamura, S.; Kimura, Y.; Oda, K.; Kawamura, K.; Sasaki, T.; Kobayashi, S.; Katayama, Y.; Ishiwata, K. *Ann. Nucl. Med.* **2008**, *22*, 151.
- Waterhouse, R. N.; Nobler, M. S.; Zhou, Y.; Chang, R. C.; Morales, O.; Kuwabara, H.; Kumar, A.; VanHeertum, R. L.; Wong, D. F.; Sackeim, H. A. *Neuroimage* **2004**, *22*, T29.
- Stone, J. M.; Arstad, E.; Erlandsson, K.; Waterhouse, R. N.; Ell, P. J.; Pilowsky, L. S. *Synapse* **2006**, *60*, 109.
- Waterhouse, R. N.; Chang, R. C.; Atuehene, N.; Collier, T. L. *Synapse* **2007**, *61*, 540.
- Shiba, K.; Ogawa, K.; Ishiwata, K.; Yajima, K.; Mori, H. *Bioorg. Med. Chem.* **2006**, *14*, 2620.
- Berardi, F.; Ferorelli, S.; Colabufo, N. A.; Leopoldo, M.; Perrone, R.; Tortorella, V. *Bioorg. Med. Chem.* **2001**, *9*, 1325.
- Moebius, F. F.; Reiter, R. J.; Hanner, M.; Glossmann, H. *Br. J. Pharmacol.* **1997**, *121*, 1.
- Moebius, F. F.; Reiter, R. J.; Bermoser, K.; Glossmann, H.; Cho, S. Y.; Paik, Y.-K. *Mol. Pharmacol.* **1998**, *54*, 591.
- Ishiwata, K.; Kawamura, K.; Yajima, K.; Tu, Q. G. L.; Mori, H.; Shiba, K. *Nucl. Med. Biol.* **2006**, *33*, 543.
- Toyohara, J.; Sakata, M.; Ishiwata, K. *Nucl. Med. Biol.* **2012**, *39*, 1049.
- Fischer, S.; Wiese, C.; Maestrup, E. G.; Hiller, A.; Deuther-Conrad, W.; Brust, P.; Liu, B.-L.; Jia, H.-M. *Bioorg. Med. Chem.* **2011**, *19*, 2911.
- Nucl. Med. Mol. Imaging **2011**, *38*, 540.
- Li, Z.-J.; Ren, H.-Y.; Cui, M.-C.; Deuther-Conrad, W.; Tang, R.-K.; Steinbach, J.; Brust, P.; Liu, B.-L.; Jia, H.-M. *Bioorg. Med. Chem.* **2011**, *19*, 2911.
- Kopka, K.; Faust, A.; Keul, P.; Wagner, S.; Breyholz, H.-J.; Höltke, C.; Schober, O.; Schäfers, M.; Levkau, B. *J. Med. Chem.* **2006**, *49*, 6704.
- Bonger, K. M.; van den Berg, R. J. B. H. N.; Heitman, L. H.; Oosterom, J.; Timmers, C. M.; Overkleef, H. S.; van der Marel, G. A. *Bioorg. Med. Chem.* **2007**, *15*, 4841.
- Kim, D. Y.; Kim, H. J.; Yu, K. H.; Min, J. J. *Bioorg. Med. Chem. Lett.* **2012**, *22*, 319.
- Kotera, N.; Delacour, L.; Traore, T.; Tassali, N.; Berthault, P.; Buisson, D.-A.; Dognon, J.-P.; Rousseau, B. *Org. Lett.* **2011**, *13*, 2153.
- Kim, Y.-S.; Yang, C.-T.; Wang, J.; Wang, L.; Li, Z.-B.; Chen, X.; Liu, S. *J. Med. Chem.* **2008**, *51*, 2971.
- Chen, R.-Q.; Li, Y.; Zhang, Q.-Y.; Jia, H.-M.; Deuther-Conrad, W.; Schepmann, D.; Steinbach, J.; Brust, P.; Wüsch, B.; Liu, B.-L. *J. Labelled Compd. Radiopharm.* **2010**, *53*, 569.
- Fan, C.; Jia, H.; Deuther-Conrad, W.; Brust, P.; Steinbach, J.; Liu, B. *Sci. China, Ser. B: Chem.* **2006**, *49*, 169.
- Kawamura, K.; Ishiwata, K.; Shimada, Y.; Kimura, Y.; Kobayashi, T.; Matsuno, K.; Homma, Y.; Senda, M. *Ann. Nucl. Med.* **2000**, *14*, 285.